

Magnetoconductivity of Hubbard bands induced in Silicon MOSFETs

T. Ferrus¹, R. George, C.H.W. Barnes, N. Lumpkin, D.J. Paul,
M. Pepper

*Cavendish Laboratory, University of Cambridge, Madingley Road, CB3 0HE,
Cambridge, United Kingdom*

Abstract

Sodium impurities are diffused electrically to the oxide-semiconductor interface of a silicon MOSFET to create an impurity band. At low temperature and at low electron density, the band is split into an upper and a lower band under the influence of Coulomb interactions. We used magnetoconductivity measurements to provide strong arguments in favour of Hubbard bands and determine the nature of the states in each band.

Key words: Silicon MOSFET, sodium, magnetoconductivity, localization, hopping, interference

PACS: 71.23.Cq, 71.55.Gs, 71.55.Jv, 72.15.Rn, 72.20.Ee, 72.80.Ng, 73.20.At, 73.40.Qv

1 Introduction

In the early 70's a substantial effort was put into the study of the effect of impurities in silicon MOSFETs. The main reason for this was to understand the origin of the observed instabilities in field effect transistors and that made unpredictable changes in the threshold voltages. These studies contributed to improve the performance of a new generation of silicon-based chips for computer applications and their degradability. Effectively, the presence of impurities or defects in the silicon oxide creates electron density inhomogeneity at the Si-SiO₂ interface and traps electrons. The most common impurities are alkali metals like lithium, potassium or sodium. These trap states give rise to

¹ E-mail : taf25@cam.ac.uk

the formation of an impurity band below the conduction band. This effect was first observed by Fang, Hartstein and Pepper [1,2,3] for high impurity concentration. A consequence of the existence of such an impurity band is that the onset voltage for conduction in oxide-doped MOSFETs is also shifted and the electron mobility substantially decreased. The impurity band produced by such a doping can be easily described by tight-binding models for high impurity density [4] whereas Mott-Hubbard models [5] need to be used for low concentration for which Coulomb interaction plays a defining role. Given single valency atoms like sodium, it would be expected that the electronic states in the band are made of single trapped electrons. However, under the influence of electron-electron interactions, it has been suggested that a stable state with two bound electrons would exist and would be characterized by a long lifetime (D_- state) [6,7]. The band formed by the D_- states is referred as the upper Hubbard band (UHB) and the one formed with neutral states as the lower Hubbard band (LHB). The question of the existence of Hubbard bands in Silicon MOSFETs has been put forward by Mott nearly thirty years ago to explain the magnetoconductivity of short disordered MOSFETs but the bands were never directly observed experimentally [8]. The study of Hubbard bands in semiconductors regained some attention since the end of the 90's with the development of quantum information and quantum computation [9]. Following the difficulty in reading out directly the value of the spin in architectures developed in agreement with the Kane model, a spin to charge conversion was proposed. This principle effectively uses a stable D_- state to perform operations. Some optical studies were carried out in Mott-Hubbard insulators like Sr_2CuO_3 [10] or boron-doped diamond [11] but no direct conductivity measurement has been performed so far. In the present paper, we used magnetoconductivity measurement to provide a direct evidence of the presence of Hubbard bands in a sodium-doped silicon MOSFET. We also describe the electronic configuration of the obtained D_- state by making the distinction between $1s^2$, $1s2s$ and $1s2p$ states.

2 Experiment

All measurements were performed on silicon MOSFETs. Such devices have been widely used because of the ability to continuously vary the electron density and the Fermi energy by use of a metal gate. The geometry of the device was chosen to be circular (Corbino geometry) to avoid leakage current paths around the source and drain contacts. The devices were fabricated using a high resistivity ($10^4 \Omega\cdot\text{cm}$) (100) p-silicon wafer to minimize as much as possible the scattering with boron acceptor impurities, especially at silicon-oxide interface. A 35 nm-gate thermal oxide was grown at 950 °C in a dry, chlorine-free oxygen atmosphere. The sidewalls of the oxide were protected by thick insulating

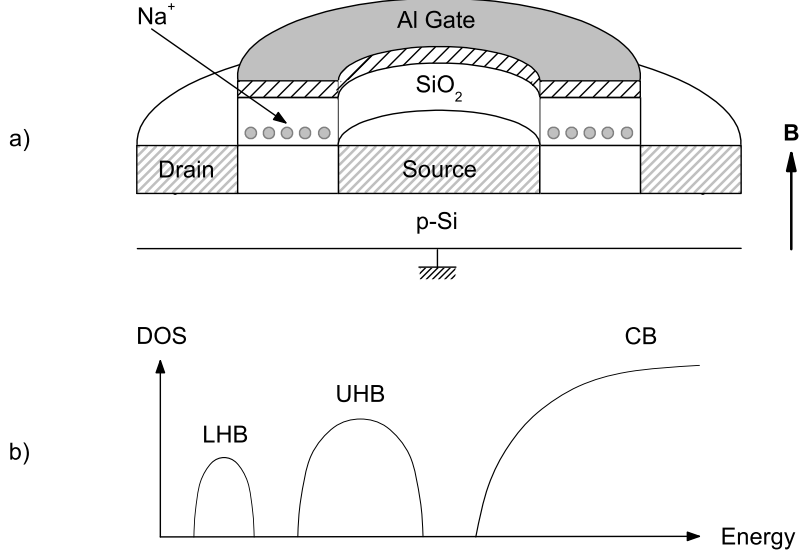


Fig. 1. a) Cross-section view of a corbino MOSFET used in the experiment when the sodium ions are close to the Si-SiO₂ interface. b) Schematic diagram of the density of states (DOS) for the present device, with a low energy (LHB) and a high energy (UHB) impurity band separated by a gap to the conduction band (CB).

LOCOS (Local Oxidation of Silicon). The effective gate length of the Corbino MOSFETs was $1\text{ }\mu\text{m}$ for an interior diameter of $110\text{ }\mu\text{m}$. Contacts were realized by implanting phosphorous at high dose and sputtering aluminium. The contact resistivity was measured to be 3.5 and $2.3\text{ }\Omega\cdot\text{cm}^{-1}$ respectively at nitrogen and helium temperatures and the sheet resistance was 6.3 and $5.9\text{ }\Omega\cdot\text{cm}^{-1}$ for the same temperatures. Sodium ions were introduced onto the oxide surface by immersing the device in a 10^{-7} N solution ($\sim 6.4\cdot 10^{11}\text{ cm}^{-2}$) of high-purity sodium chloride in deionized water. The surface of the chip was then dried with nitrogen gas and an aluminium gate subsequently evaporated. The application of a positive gate voltage ($+4\text{ V}$ at 65°C for 10 mins) causes the sodium ions to drift towards the Si-SiO₂ interface while the application of -4 V dc in the same conditions removes the ions from the interface. The ions are frozen at their position once the device temperature becomes lower than 150 K (Fig.1). Standard low-noise lock-in techniques with an amplifier of 10^8 V/A were used to measure the source to drain conductivity. An ac excitation of amplitude $V_{ac} = 15\text{ }\mu\text{V}$ and a frequency of 11 Hz were chosen. The dc offset of the amplifier was cut using appropriate RC filters. The gate voltage was controlled by a high resolution digital to analog converter and the temperature measured by a calibrated germanium thermometer. The magnetic field was produced by an Oxford 12 T superconducting magnet and applied perpendicular to the Si-SiO₂ interface.

Several devices were processed identically and gave results that lead to identical conclusions although we noticed some variations in the relative positions and in the widths of impurity bands as well as in the conductivity values. We

also fabricated a number of control devices that were not exposed to sodium contamination and were used for comparison. The following results are presented for a specific device that was chosen for its high reproducibility in time as well as for its low noise to signal ratio.

3 Results and discussion

Fig. 2a represents the source-drain conductivity obtained at different values of the magnetic field. The dependence of conductivity in temperature on the same device in the hopping regime showed the presence of two groups of peaks clustered around $V_g = -2$ and -0.5 V. They were attributed to a split impurity band due to the presence of sodium impurity at the Si-SiO₂ interface [12]. Arguments in favour for Hubbard bands were then provided while studying the variation of conductivity at higher temperature where activation mechanisms take place. [13]

The magnetoconductivity is found to be negative for the all range of gate voltages studied as this is expected and was already observed in localized systems [14,15,16] (Fig. 2b). Its variation with magnetic field is well described by $\ln \sigma \sim -\alpha B^2$ even at fields up to 5 T. This behaviour is often attributed to the presence of forward scattering paths formed when the field-induced compression of the donor wavefunctions is sufficient to reduce significantly the wavefunction overlap between neighbouring sites and increase the localization of electrons [17]. The wavefunction then acquires a phase factor $\phi \sim \xi r^3 / l_B^4$ where l_B is the magnetic length given by $l_B = (\hbar / eB)^{1/2}$, r the hopping length and ξ is the localization length. This supposes a gaussian distribution for the flux ϕ . For transport processes involving only one hop within an area $(\xi r^3)^{1/2}$ like the nearest-neighbour hopping or resonant tunneling, $\ln \sigma$ is found to be quadratic in magnetic field with α given by : [18]

$$\alpha = \frac{1}{12} \left(\frac{B_c}{\pi} \right)^{1/2} \frac{e^2 \xi}{\hbar^2 N_T^{3/2}} \quad (1)$$

N_T is the density of active traps and B_c is a constant describing the number of bonds in a circular percolation problem, being π in tunnelling problems and respectively 4.5 and 2.7 in the case of nearest-neighbour hopping in a zero or finite width impurity band. If, however, the transport is described by several hops, a minimization procedure as first used by Mott [19] needs to be realized in order to find the optimum hopping length and hopping energy. This makes α temperature dependent [20].

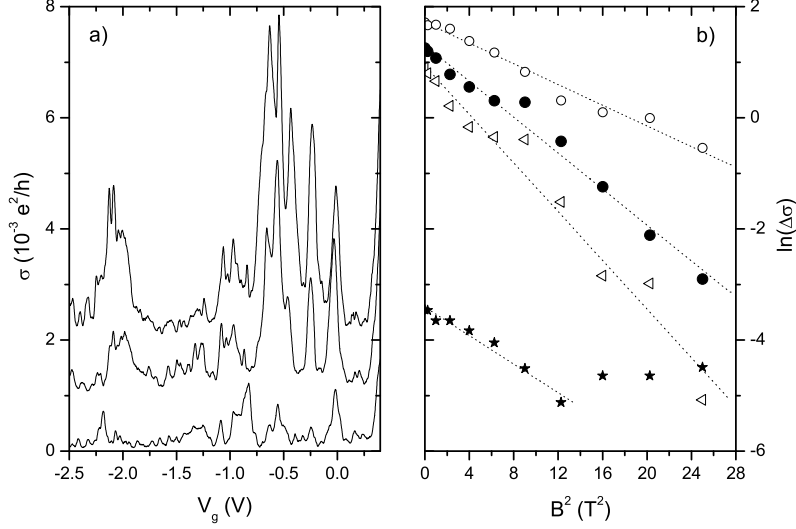


Fig. 2. a) Conductivity versus gate voltage at $B = 0$ T, 2.5 T and 5 T (from top to bottom) at 309 mK. For clarity curves are separated by a constant offset of $10^{-3} e^2/h$. b) Magnetoconductivity for $V_g = -0.24$ (○), -0.56 (●), -0.97 V (★) and -2.08 V (◁).

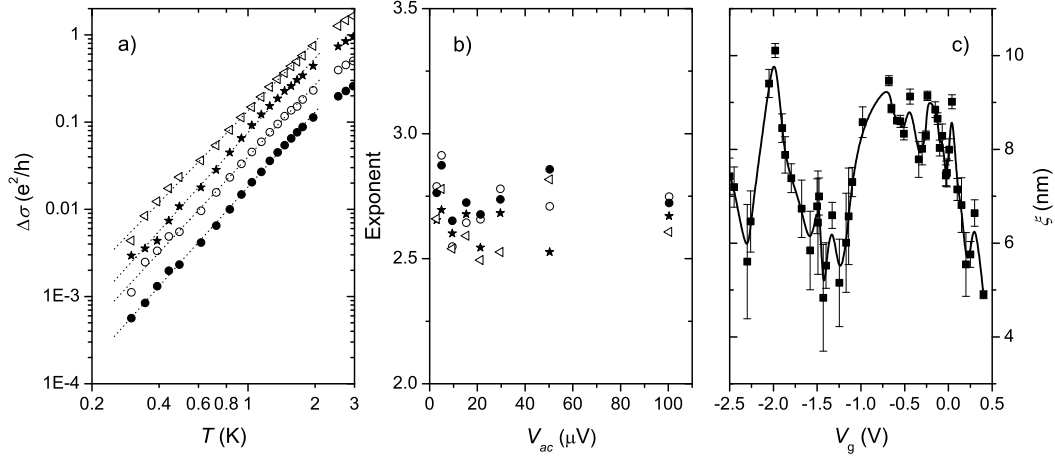


Fig. 3. a) Variation of the conductivity in temperature for $V_g = -0.24$ (○), -0.56 (●), -0.97 V (★) and -2.08 V (◁). b) Variation of the temperature exponent with V_{ac} at the same gate voltages. c) Variation of the localization length in terms of V_g at 309 mK deduced from Eq. 3.

$$\alpha = \frac{1}{24} \frac{e^2 \xi^4}{\hbar^2} \frac{1}{(p+3)^3} \left(\frac{T_0}{T} \right)^{3 \left(\frac{p+1}{p+3} \right)} \quad (2)$$

where p is 0 in case of the Mott variable range hopping regime [21] or 1 in case electron correlations are important (Efros and Shklovskii regime [22])

The proper analysis of $\sigma(B)$ is thus constrained to the correct description of the transport mechanism at low temperature. Below 1 K, the conductivity de-

creases rapidly with temperature as $\Delta\sigma = \sigma(T) - \sigma(0) \sim T^{2.7}$ (Fig. 3a). This variation is not affected by the source-drain voltage and $eV_{ac} < k_B T$ in all measurements (Fig 3b). Consequently, we do not expect this results from electron heating in the contacts but from a contribution of the acoustic phonons at low temperature. In our previous study, the same data were analyzed in temperature and we showed the transport was characterized by hopping conduction with an exponent $p \sim 0.4$ above 1 K [12]. In the framework of 2D resistance networks [23] the conductivity is $\sigma \sim \nu/T$ whereas the scattering time is $\tau \sim \nu r^2/T$ where ν is the hopping rate and r the hopping length. Our results showed the best fits were obtained with an exponential prefactor $\sim T^{-0.8}$. This implies τ varies as $T^{-1.6}$. This value is close to the $T^{-3/2}$ law expected in non-polar semiconductor for acoustic phonon scattering [24] and as it was observed in Silicon [25]. The excellent agreement with theory implies that acoustic phonon-assisted hopping was the main mechanism for transport above 1 K and that this transport is in fact still active and predominant at 300 mK. Moreover, we found that $r \sim 3\xi$. This indicates that a few hops are necessary between the initial and the final states. Consequently, Eq. 3 should be used with $p = 0.4$ to estimate the value of the localization length ξ at low temperature, obtaining the values of T_0 from our previous analysis [12]. Results are shown on Fig. 3c. The variation of $\xi(V_g)$ is consistent with our previous observations, i.e. an increase of the localization at the band positions, but the values are here nearly half of those obtained from $T_0(\xi)$ in the absence of magnetic field [12]. Such a halving of ξ has already been observed experimentally in insulating devices with strong spin-orbit coupling [31]. It is plausible that such an effect takes place in our device because of the presence of potential fluctuations at the Si-SiO₂ interface. We also observed the conductivity of the lower band is suppressed at around 3.5 T whereas the upper band is still conducting even at the higher field. This suggests that the lower band is energetically deeper and already strongly localized even in the absence of magnetic field. Effectively, the upper band is supposed to be closer to the extended states in energy than the lower band and it is likely to be more deeply influenced by the enhancement of the localization due to the shrinkage of the electron wave function caused by the magnetic field.

We also observed a non-monotonic decrease of the conductivity with magnetic field. This takes the form of fluctuations which amplitude varies with gate voltage. These fluctuations are present in many of our devices except for devices with no sodium ions. They may appear as a series of positive and negative magnetoconductivities. Their position in magnetic field may also change with time but their general characteristics is a periodicity in B . Such fluctuations have already been observed by Nguyen [26] and may be attributed to random interference between different tunneling paths in magnetic field. To proceed with the analysis, the position B_m in field of the fluctuation extrema were extracted from the curve $\Delta\sigma(B) = \sigma(B) - \sigma_0 \exp(-\alpha B^2)$ and plotted as a function of the extrema index (Figure 4). We found a linear dependence

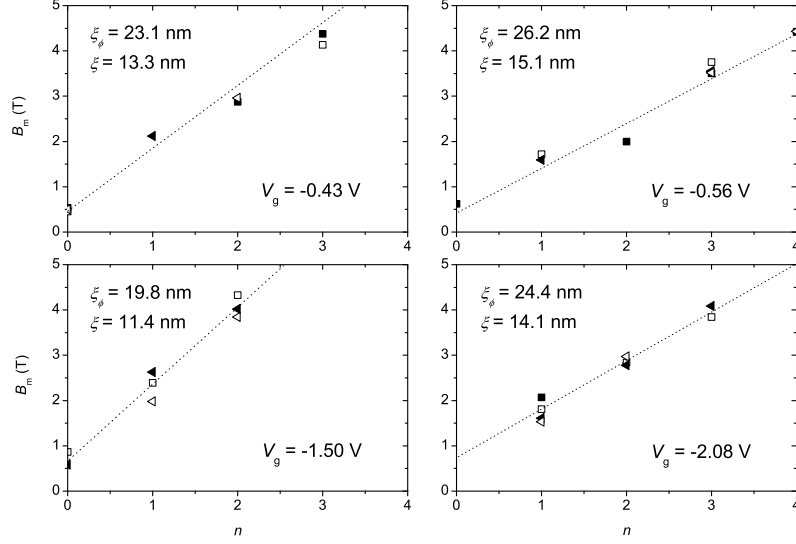


Fig. 4. Measure of the critical field of the fluctuations and the corresponding values ξ_ϕ and ξ for $V_g = -0.43$ (○), -0.56 (●), -1.50 V (★) and -2.08 V (◁) at 309 mK.

with a slope B_ϕ for all gate voltages indicating the fluctuations are periodic in magnetic field. To minimize the uncertainty due to the limited number of points, the experiment was repeated four times with the same configuration. We found that $\xi_\phi = (\hbar/eB_\phi)^{1/2} \leq \xi$ but $\xi_\phi \sim (r\xi)^{1/2}$. We can deduce the modulation correspond to an integer of elementary flux in a surface of $\pi r\xi$ and that B_ϕ is given by :

$$B_c = \frac{nh}{2\pi er\xi} \quad (3)$$

This situation is similar to the one explaining Aharonov-Bohm oscillations in quantum dots systems [27] with $(r\xi)^{1/2}$ playing the role of the dot radius. In the hopping regime, the interference area has a cigar-shape with radius ξ in one direction and the hopping length in the hop direction. Quantum interferences between forward and backscattering paths induced by localizing impurity potential in magnetic field may be responsible for such fluctuations. Finally, we should discuss about the variation of the position of the peaks in magnetic field (Fig.5). We observed the group of peaks clustered in the upper band moves linearly with magnetic field with a slope of ~ -4 mV/T whereas the one in the lower band move with a slope of $\sim +4$ mV/T. Movements of energy levels are expected in magnetic field but the difference in the sign can only be explained by including the effect of the orbital momentum. By considering the electrons are localized at the impurity sites with an approximate parabolic potential of width ω_0 , the variation ΔE of an energy level is described by [29,30]:

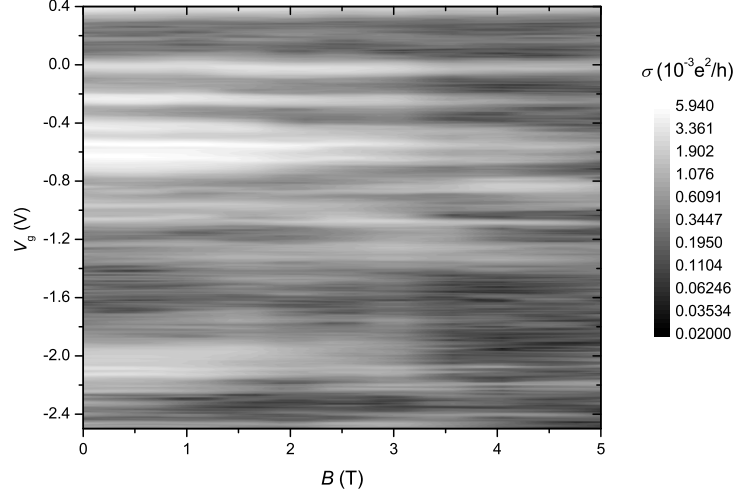


Fig. 5. Conductivity versus gate voltage and magnetic field at 309 mK.

$$\Delta E = (2n + |l| + 1) \hbar \left[\sqrt{\frac{\omega_c^2}{4} + \omega_0^2} - \omega_0 \right] - \frac{1}{2} l \hbar \omega_c \quad (4)$$

where n is the index for the Landau level, l is the value of the angular momentum and $\omega_c = eB/m^*$ with $m^* = 0.19 m_e$ the effective mass of the electrons in silicon.

Consequently, $n = 0$ and $l = 0$ are associated with the lower group of peaks (non-degenerated) and $n = 1$ and $l = 1$ to the upper group (twice-degenerated). The value $l = 1$ also indicate the necessary presence of two electrons in the configuration 1s2p. This gives credit to the formation of Hubbard bands [28] and a stable Na^- ion at the Si-SiO₂ interface as well as the presence of a strong spin-orbit coupling. This shows as well the importance of Coulomb interactions in this system. When increasing the magnetic field, the wave-function of the lowest state shrinks and the interaction between the two degenerate electrons grows until the Zeeman energy is sufficient to spin-flip the second electron and promote it to the $l = 1$ state. This transition is predominantly caused by Coulomb interactions since no spin splitting was observed and was still quite small even at 5 T. Finally, the 1s2p configuration holds as long as $\Delta E < 0$ for the upper band which is verified up to 5 T. This implies that $\hbar\omega_0 > 2.7 \text{ meV}$ and provides a lower bound for the mean impurity potential depth.

4 Conclusion

We have observed a negative magneto-conductivity up to 5 T. This result confirms the previous observations done on the same device that the system is strongly localized with a localization length of the order of the mean distance between impurities. The fluctuations observed in the conductivity have been attributed to quantum interference due by the presence of impurity centres close to the interface in presence of magnetic field. Finally, the shift in the position of the upper and lower bands are compatible with the presence of an upper and lower Hubbard bands and a possible transition from a singlet to a triplet state in the upper band induced by electron-electron interaction.

Acknowledgement

We would like to thank Drs T. Bouchet and F. Torregrossa from Ion Beam System-France for the process in the device as well as funding from the U.S. ARDA through U.S. ARO grant number DAAD19-01-1-0552.

References

- [1] F. F. Fang and A. B. Fowler, Phys. Rev. 169, 619 (1967)
- [2] A. Hartstein and A. B. Fowler, Phys. Rev. Lett. 34, 1435 (1975)
- [3] M. Pepper, J. Phys. C : Solid State Phys., 10, L173 (1977)
- [4] A. P. Sutton, M. W. Finnis, D. G. Pettifor and Y Ohta , J. Phys. C : Solid State Phys., 21, 35 (1988)
- [5] J. Hubbard, Proc. Roy. Soc. A 276 238 (1963)
- [6] P. Norton, Phys. Rev. Lett. 37, 164 (1976)
- [7] M. Taniguchi and S. Narita, Solid State Comm. 20, 131 (1976)
- [8] A. B. Fowler, J. J. Wainer and R. A. Webb, IBM J. Res. Develop., 32, 372 (1988)
- [9] B.E. Kane, Nature 393, 133 (1998)
- [10] H. Kishida, H. Matsuzaki, H. Okamoto, T. Manabe, M. Yamashita, Y. Taguchi and Y. Tokura, Nature 405, 929 (2000)
- [11] Dan Wu, Y. C. Ma, Z. L. Wang, Q. Luo, C. Z. Gu, and N. L. Wang, C. Y. Li, X. Y. Lu and Z. S. Jin, Phys. Rev. B 73,012501 (2006)

- [12] T. Ferrus et al, Phys. Rev. B 73, 4, 041304 (2006)
- [13] T. Ferrus et al, cond-mat/0512039 (2006)
- [14] A. Ghosh, M. Pepper, H. E. Beere and D. A. Ritchie, Phys. Rev. B 70, 233309 (2004)
- [15] G. Timp and A. B. Fowler, Phys. Rev. B 33, 4392 (1986)
- [16] H. Reisinger, A. B. Fowler and A. Hartstein, Surf. Sci. 142, 274 (1984)
- [17] B. I. Shklovskii and A. L. Efros, in Electronic properties of doped semiconductors, Springer series in solid-state sciences, No 45, Springer Berlin (1984)
- [18] V. L. Nguen, Sov. Phys. Semicond 18 (2), 207 (1984)
- [19] N. H. Mott, J. Non-Cryst. Solids 1, 1 (1968)
- [20] B. I. Shklovskii, Fiz. Tekh Poluprovodn. (S.-Petersburg) 17, 2055 (1983) [Sov. Phys. Semicond. 17, 1311 (1983)]
- [21] N. F. Mott and E. A. Davis, Electronic Processes in Non-Crystalline Materials, 2nd ed. (Oxford University Press, London, 1979)
- [22] A. L. Efros and B. I. Shklovskii, J. Phys. C: Solid State Phys. 8, L49 (1975)
- [23] A. Miller and E. Abrahams, Phys. Rev. 120, 745 (1960)
- [24] J. Bardeen and W. Shockley, Phys. Rev. 80, 1, 72 (1950)
- [25] M. B. Prince, Phys. Rev. 93, 6, 1204 (1954)
- [26] Nguyen, Sov. Phys. JETP 62, 1021 (1986)
- [27] R. A. Webb, S. Washburn, C. P. Umbach and R. B. Laibowitz, Phys. Rev. Lett. 54, 2968 (1988)
- [28] P. Norton, Phys. Rev. Lett. 37, 164 (1976)
- [29] V. Fock, Z. Phys. 47, 446 (1928)
- [30] C.G. Darwin, Proc. Cambridge Philos. Soc. 27, 86 (1930)
- [31] J. L. Pichard, M. Sanquer, K. Slevin and P Debray, Phys. Rev. Lett. 65, 1812 (1990)